This article was downloaded by: [University of Toledo], [K. A. Shamaileh]
On: 24 January 2014, At: 09:18
Publisher: Taylor & Francis
Informa Ltd Registered in England and Wales Registered Number: 1072954 Registered office: Mortimer House, 37-41 Mortimer Street, London W1T 3JH, UK

Electromagnetics
Publication details, including instructions for authors and subscription information:
http://www.tandfonline.com/loi/uemg20

Realization of Multi-Band 3-dB Branch-Line Couplers Using Fourier-Based Transmission Line Profiles

K. A. Shamaileh [a], M. J. Almalkawi [a], V. K. Devabhaktuni [a], N. I. Dib [b] & S. Abushamleh [c]

[a] Electrical Engineering and Computer Science Department, University of Toledo, Toledo, Ohio, USA

[b] Electrical Engineering Department, Jordan University of Science and Technology, Irbid, Jordan

[c] Department of Systems Engineering, University of Arkansas at Little Rock, Arkansas, USA

Published online: 24 Jan 2014.

To cite this article: K. A. Shamaileh, M. J. Almalkawi, V. K. Devabhaktuni, N. I. Dib & S. Abushamleh (2014) Realization of Multi-Band 3-dB Branch-Line Couplers Using Fourier-Based Transmission Line Profiles, Electromagnetics, 34:2, 128-140

To link to this article: http://dx.doi.org/10.1080/02726343.2014.863686

PLEASE SCROLL DOWN FOR ARTICLE

Taylor & Francis makes every effort to ensure the accuracy of all the information (the "Content") contained in the publications on our platform. However, Taylor & Francis, our agents, and our licensors make no representations or warranties whatsoever as to the accuracy, completeness, or suitability for any purpose of the Content. Any opinions and views expressed in this publication are the opinions and views of the authors, and are not the views of or endorsed by Taylor & Francis. The accuracy of the Content should not be relied upon and should be independently verified with primary sources of information. Taylor and Francis shall not be liable for any losses, actions, claims, proceedings, demands, costs, expenses, damages, and other liabilities whatsoever or howsoever caused arising directly or indirectly in connection with, in relation to or arising out of the use of the Content.

This article may be used for research, teaching, and private study purposes. Any substantial or systematic reproduction, redistribution, reselling, loan, sub-licensing, systematic supply, or distribution in any form to anyone is expressly forbidden. Terms &

Conditions of access and use can be found at http://www.tandfonline.com/page/terms-and-conditions

Downloaded by [University of Toledo], [K. A. Shamaileh] at 09:18 24 January 2014

Electromagnetics, 34:128–140, 2014
Copyright © Taylor & Francis Group, LLC
ISSN: 0272-6343 print/1532-527X online
DOI: 10.1080/02726343.2014.863686

Downloaded by [University of Toledo], [K. A. Shamaileh] at 09:18 24 January 2014

Realization of Multi-Band 3-dB Branch-Line Couplers Using Fourier-Based Transmission Line Profiles

K. A. SHAMAILEH,[1] M. J. ALMALKAWI,[1]
V. K. DEVABHAKTUNI,[1] N. I. DIB,[2] and
S. ABUSHAMLEH[3]

[1]Electrical Engineering and Computer Science Department, University of Toledo, Toledo, Ohio, USA
[2]Electrical Engineering Department, Jordan University of Science and Technology, Irbid, Jordan
[3]Department of Systems Engineering, University of Arkansas at Little Rock, Arkansas, USA

Abstract *A new procedure for the design of multi-band branch-line couplers utilizing microstrip non-uniform transmission lines with Fourier-based profiles is presented in this article. The general method is accomplished by replacing the quarter-wave uniform transmission lines of a conventional coupler with multi-band non-uniform transmission lines of the same lengths, without including additional transmission lines or matching networks. The design of non-uniform transmission line couplers is performed using even- and odd-mode analysis. The proposed structure is relatively simple and is fabricated on a single-layered microstrip board. Two design examples of dual- and triple-band branch-line couplers suitable for global system mobile (GSM), wireless local area networks, and WiFi communications are designed, fabricated, and experimentally evaluated to validate the proposed methodology.*

Keywords branch-line coupler, Fourier, microstrip, multi-band 3-dB couplers, non-uniform transmission line

1. Introduction

Microwave couplers are essential components for a host of system applications, such as modern radar, test equipment, and RF mixers, where reduced-size circuitry and multi-frequency operation are two main requirements. The quadrature branch-line coupler (BLC) is a well-known component that has been extensively addressed in the literature due to its wide use in microwave subsystems. However, the inherent single-frequency matching nature of conventional couplers that are based on quarter-wave transmission lines limits its applications to multi-band systems. Normally, dual-frequency

Received 3 May 2013; accepted 4 August 2013.
Address correspondence to K. A. Shamaileh, Electrical Engineering and Computer Science Department, University of Toledo, Toledo, OH 43606. E-mail: Khair.Alshamaileh@utoledo.edu
Color versions of one or more of the figures in the article can be found online at www.tandfonline.com/uemg.

Downloaded by [University of Toledo], [K. A. Shamaileh] at 09:18 24 January 2014

characteristics are achieved through the use of dual-band quarter-wavelength impedance transformers (Cheng & Yeung, 2012) attained by the proper selection of the circuit parameters. Nevertheless, the increase in the circuitry size is a major concern for such an approach and may not be an option for given design constraints.

Another way to realize the dual-band characteristics of BLCs is either by (a) using unequal arms lengths and a center-tapped stub (Park, 2009); (b) incorporating stepped-impedance stubs placed at the middle of each quarter-wave arm of the conventional coupler (Chin et al., 2010); (c) using four open-ended quarter-wave transmission lines at each port of the conventional BLC (Cheng & Wong, 2004), where the lengths of the additional stubs as well as the main arms are evaluated at the middle frequency of the two operating bands; or (d) employing three coupled-line sections, as demonstrated in Yeung (2011). Lin et al. (2010) proposed a tri-band BLC with three controllable operating frequencies employing four matching stubs at each port. A similar technique was developed in Tanigawa et al. (2007), for which triple-broadband matching techniques employing matching stubs were considered in the design of a 3-dB BLC. A tri-band BLC using double-Lorentz transmission lines was introduced in Lee and Nam (2007), where lumped capacitors and inductors were incorporated in the middle of each arm of a conventional BLC, and the design of a tri-band coupler for WiMAX applications was investigated in Sinchangreed et al. (2011).

The lack of detailed design procedure and analysis, however, makes the design of such multi-band couplers a difficult task. Recently, triple- and quad-band 3-dB couplers were proposed by adopting optimized compensation techniques to satisfy the matching conditions (Liou et al., 2009; Piazzon et al., 2012). It is worth pointing out that multi-band couplers in Cheng and Yeung (2012), Park (2009), Chin et al. (2010), Cheng and Wong (2004), Yeung (2011), Lin et al. (2010), Tanigawa et al. (2007), Sinchangreed et al. (2011), and Piazzon et al. (2012) were realized by adding extra transmission lines and/or matching stubs, which remarkably increases the overall circuit size; however, in Lee and Nam (2007), lumped elements were incorporated in the design. Typically, single-stage couplers exhibit narrowband frequency characteristics, and broader bandwidth is achieved by using cascaded couplers (Jung et al., 2009) or broadband matching techniques (Tanigawa et al., 2007) that are beyond the scope of this work.

In this article, equally split dual- and triple-band BLCs based on non-uniform transmission lines (NTLs) are proposed. Practical frequencies are chosen as design frequencies for two examples. In addition to the excellent electrical performance of the input port matching, isolation, transmission, and coupling characteristics at each design frequency in both couplers, no extra matching stubs are included in the design. As such, no extra circuit area is required.

The organization of this article is as follows: Section 2 presents the proposed step-by-step procedure of the multi-band 3-dB BLCs. Section 3 discusses the implementation of two design examples, including dual- and triple-band BLCs, and reports their measured performances, while conclusions are presented in Section 4.

2. Multi-Band 90° BLC Design

In this section, the theory of designing multi-band BLCs utilizing NTLs is presented. Figure 1 shows the proposed multi-band BLC, which consists of six variable profile impedances formed from $Z_1(z)$ and $Z_2(z)$ with lengths d_1 and d_2, respectively, while Figure 2 illustrates the corresponding even- and odd-mode circuits.

Downloaded by [University of Toledo], [K. A. Shamaileh] at 09:18 24 January 2014

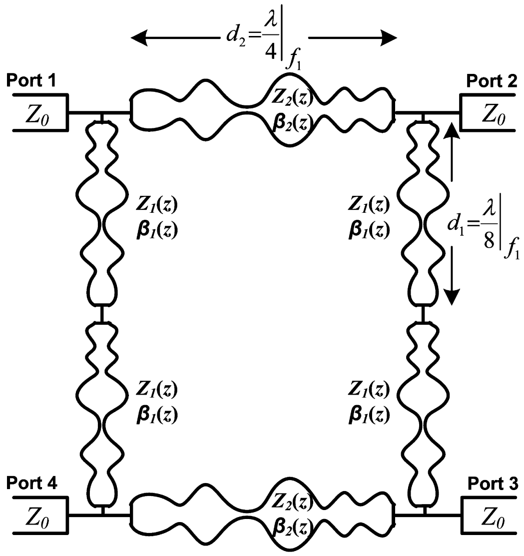

Figure 1. Schematic diagram for proposed NTL multi-band BLC.

Referring to Figure 2, the total $ABCD$ matrix of the whole design can be found by multiplying the $ABCD$ parameters of each individual arm, described by:

$$\begin{bmatrix} A & B \\ C & D \end{bmatrix}_{even} = \begin{bmatrix} 1 & 0 \\ \left(Z_{in}^{even}\right)^{-1} & 1 \end{bmatrix} \begin{bmatrix} A & B \\ C & D \end{bmatrix}_{Z_2(z)} \begin{bmatrix} 1 & 0 \\ \left(Z_{in}^{even}\right)^{-1} & 1 \end{bmatrix}, \tag{1a}$$

$$\begin{bmatrix} A & B \\ C & D \end{bmatrix}_{odd} = \begin{bmatrix} 1 & 0 \\ \left(Z_{in}^{odd}\right)^{-1} & 1 \end{bmatrix} \begin{bmatrix} A & B \\ C & D \end{bmatrix}_{Z_2(z)} \begin{bmatrix} 1 & 0 \\ \left(Z_{in}^{odd}\right)^{-1} & 1 \end{bmatrix}. \tag{1b}$$

The $ABCD$ parameters of the non-uniform impedance profile $Z_j(z)$ $(j = 1, 2)$ can be determined by subdividing such an impedance into K uniform electrically short segments,

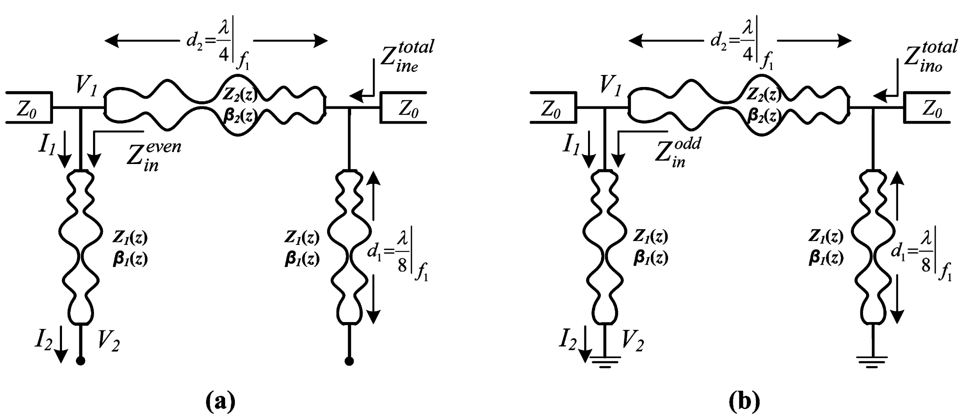

Figure 2. Proposed non-uniform BLC: (a) even-mode circuit and (b) odd-mode circuit.

Downloaded by [University of Toledo], [K. A. Shamaileh] at 09:18 24 January 2014

each with length Δz. The $ABCD$ parameters of the overall arm $Z_j(z)$ are then obtained by multiplying the $ABCD$ parameters of each section as follows (Pozar, 2005):

$$\begin{bmatrix} A & B \\ C & D \end{bmatrix}_{Z_j(z)} = \begin{bmatrix} A_1 & B_1 \\ C_1 & D_1 \end{bmatrix} \cdots \begin{bmatrix} A_i & B_i \\ C_i & D_i \end{bmatrix} \cdots \begin{bmatrix} A_K & B_K \\ C_K & D_K \end{bmatrix}. \tag{2}$$

where the $ABCD$ parameters of the ith segment are (assuming lossless transmission lines) (Pozar, 2005):

$$A_i = D_i = \cos(\Delta\theta), \tag{3a}$$

$$B_i = Z^2((i-0.5)\Delta z)C_i = jZ((i-0.5)\Delta z)\sin(\Delta\theta), \qquad i = 1, 2, \ldots, K, \tag{3b}$$

$$\Delta\theta = \frac{2\pi}{\lambda}\Delta z = \frac{2\pi}{c} f\sqrt{\varepsilon_{eff}}\Delta z. \tag{3c}$$

The effective dielectric constant ε_{eff} of each section is calculated using the well-known microstrip line formulas given in Pozar (2005). Then, the total uniformly subdivided microstrip sections that form the characteristic impedance $Z_j(z)$ are approximated by means of a truncated Fourier series with unknown coefficients (Khalaj-Amirhosseini, 2006; 2008):

$$\ln\left(\frac{Z_j(z)}{Z_{oj}}\right) = \sum_{n=0}^{N} C_n \cos\left(\frac{2\pi n z}{d_j}\right). \tag{4}$$

The microstrip line lengths d_1 and d_2 are chosen to be $\lambda/8$ and $\lambda/4$, respectively, at the lowest design frequency f_1. These wavelengths are those corresponding to uniform microstrip lines with impedances of 50 and 35 Ω. The characteristic impedances, Z_{o1} and Z_{o2}, are equal to 50 and 35 Ω, respectively, and N is the number of the Fourier series coefficients. Moreover, $Z_j(z)$ must be restricted by constraints that allow practical realization and easy fabrication for the proposed couplers, as follows:

$$\overline{Z}_{\min} \le \overline{Z}_j(z) \le \overline{Z}_{\max}, \tag{5a}$$

$$\overline{Z}_j(0) = \overline{Z}_j(d_j) = 1. \tag{5b}$$

Upon determining the $ABCD$ parameters of $Z_1(z)$ by following the design equations (Eqs. (2) through (5b)), the following equation can be written as:

$$\begin{bmatrix} V_1 \\ I_1 \end{bmatrix} = \begin{bmatrix} A & B \\ C & D \end{bmatrix}_{Z_1(z)} \begin{bmatrix} V_2 \\ I_2 \end{bmatrix}. \tag{6}$$

Setting I_2 in Eq. (6) to zero, and solving for $\frac{V_1}{I_1}$, one obtains:

$$\frac{V_1}{I_1} = \frac{A}{C} = Z_{in}^{even}. \tag{7}$$

Similarly, the odd-mode input impedance Z_{in}^{odd} shown in Figure 2(b) can be determined by setting V_2 in Eq. (6) to zero, leading to:

$$\frac{V_1}{I_1} = \frac{B}{D} = Z_{in}^{odd}. \tag{8}$$

Consequently, the $ABCD$ matrices for the circuit modes shown in Figure 2 are calculated using Eqs. (1a) and (1b), where the non-uniform impedance $Z_2(z)$ is determined by following the design equations (Eqs. (2) through (5b)). Thus, the total input impedance for each mode can be expressed by the following equation (Pozar, 2005):

$$Z_{in_{e,o}}^{total} = \frac{A_{e,o}Z_o + B_{e,o}}{C_{e,o}Z_o + D_{e,o}}, \tag{9}$$

where Z_o is the characteristic impedance of each feed port. Here, the procedure carried out in Eqs. (1a) to (9) is followed for each design frequency f_m $(m = 1, 2, \ldots, M)$. Thus, the reflection and transmission coefficients for the NTL BLC can be written as (Pozar, 2005):

$$\Gamma_{e,o}(f_m) = \frac{Z_{in_{e,o}}^{total} - Z_o}{Z_{in_{e,o}}^{total} + Z_o}, \tag{10a}$$

$$T_{e,o}(f_m) = \frac{2}{A_{e,o} + \dfrac{B_{e,o}}{Z_o} + C_{e,o}Z_o + D_{e,o}}. \tag{10b}$$

The S-parameters for the NTL BLC can be calculated using the following equations (Pozar, 2005):

$$S_{11}(f_m) = \frac{\Gamma_e(f_m) + \Gamma_o(f_m)}{2}, \tag{11a}$$

$$S_{41}(f_m) = \frac{\Gamma_e(f_m) - \Gamma_o(f_m)}{2}, \tag{11b}$$

$$S_{21}(f_m) = \frac{T_e(f_m) + T_o(f_m)}{2}, \tag{11c}$$

$$S_{31}(f_m) = \frac{T_E(f_m) - T_o(f_m)}{2} \tag{11d}$$

Finally, to obtain the desired response at the design frequencies, the optimum values of the Fourier coefficients C_n can be obtained through minimizing the following error function:

$$E(f_1, \ldots, f_M) = \sqrt{\frac{|S_{11}|^2 + |S_{41}|^2 + \left||S_{21}|^2 - |S_{21}|_{des}^2\right| + \left||S_{31}|^2 - |S_{31}|_{des}^2\right|}{16M}}, \tag{12}$$

where $|S_{21}|_{des} = |S_{31}|_{des} = 0.707$, and M corresponds to the number of design frequencies. The term $16M$ in the denominator acts as a normalization factor; the error function in Eq. (12) can be formulated in several ways to achieve the design goals. To solve such a constrained optimization problem, a trust-region-reflective algorithm (Li,

Downloaded by [University of Toledo], [K. A. Shamaileh] at 09:18 24 January 2014

1993) is adopted that can solve large-scale bound-constrained non-linear minimization problems with strong convergence properties. Figure 3 shows a flowchart summarizing the design procedure described by Eqs. (1) through (12). In the optimization process, there is no unique solution for the unknown Fourier coefficients values, and each optimization run results in a different set. However, the one that gives the optimal response accompanied with an impedance profile that is realizable and complies with Eqs. (5a) and (5b) is considered in the further design steps. Furthermore, the design principle can be

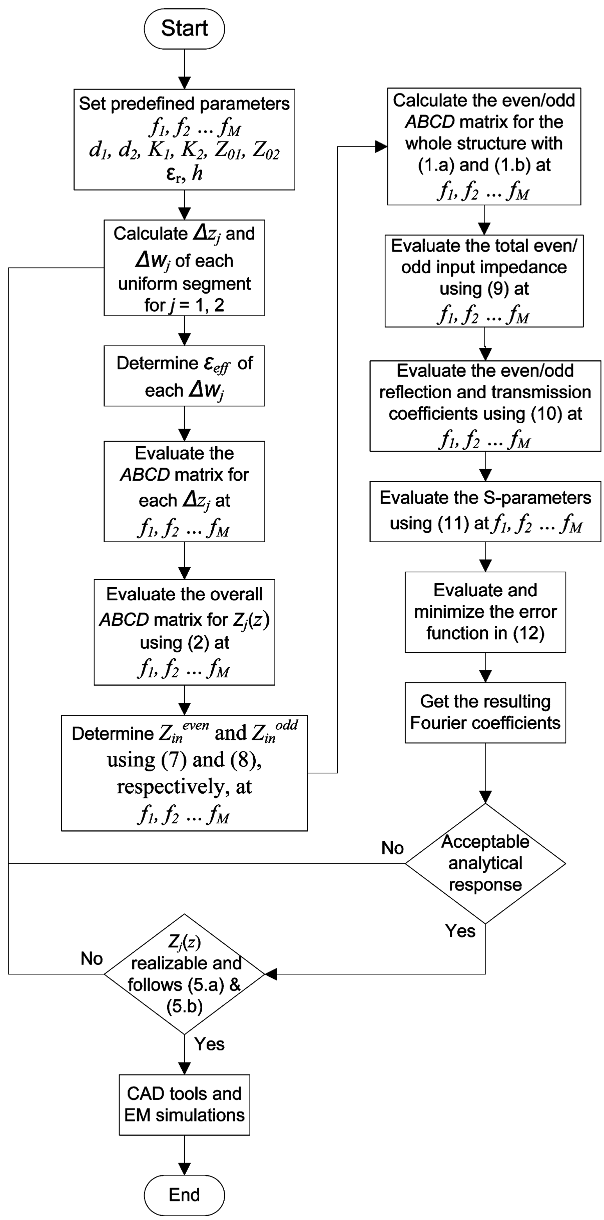

Figure 3. Flowchart demonstrating general design procedure of multi-band non-uniform BLC.

Downloaded by [University of Toledo], [K. A. Shamaileh] at 09:18 24 January 2014

generalized to design BLCs of an unequal split type, taking into account proper values of the branches impedances (see Rawat et al. [2013] and the references therein).

3. Design Examples

Two design examples of dual- and triple-band BLCs are presented in this section to validate the design procedure proposed in Section 2. For justification, the proposed designs are simulated using two different full-wave electromagnetic simulators, namely IE3D (Mentor Graphics PCB Design Software, 2006) and HFSS (Ansys, Inc., 2011), which are based on the method of moments (MoM) and the finite-element method (FEM), respectively. For further validation, the presented examples are also fabricated and tested considering a Rogers RO4835 substrate with a relative permittivity of 3.48, loss tangent of 0.0037, substrate thickness of 1.524 mm, and copper clad thickness of 17 μm.

3.1. Dual-Band 3-dB BLC

Considering the design steps demonstrated in Figure 3, a dual-frequency NTL BLC with design frequencies chosen to be 0.9 and 2.4 GHz is presented. The 0.9 GHz frequency band is widely used in global system mobile (GSM) technology, whereas the 2.4 GHz band fits in many wireless applications, such as IEEE 802.11b,g,n standards (wireless local area network [WLAN] and/or WiFi). In the dual-band BLC example, two NTLs—$Z_1(z)$ and $Z_2(z)$, with widths 2.5 mm $< W_1(z) <$ 5 mm and 2 mm $< W_2(z) <$ 12 mm, respectively—are designed with lengths d_1 and d_2 of 25.18 and 49.27 mm, respectively, whereas the characteristic impedances Z_{o1}, Z_{o2}, and Z_o are chosen to be 50, 35, and 50 Ω, respectively. K_1, K_2, and N are set to 50, 50, and 10, respectively, and the resulting error value from the optimization process was 0.022. Table 1 shows the obtained Fourier series coefficients for $Z_1(z)$ and $Z_2(z)$.

Table 1
Fourier coefficients for variable impedance profiles in dual-band BLC design

Fourier coefficients for $Z_1(z)$					
C_0	C_1	C_2	C_3	C_4	C_5
0.0534	–0.0923	0.0102	0.0057	0.0043	0.0036
C_6	C_7	C_8	C_9	C_{10}	
0.0036	0.0033	0.0031	0.0030	0.0029	0.0028
Fourier coefficients for $Z_2(z)$					
C_0	C_1	C_2	C_3	C_4	C_5
–0.0370	–0.1661	–0.3631	0.3822	0.0916	0.0567
C_6	C_7	C_8	C_9	C_{10}	
0.0193	0.0112	0.0044	0.0016	–0.0008	

Downloaded by [University of Toledo], [K. A. Shamaileh] at 09:18 24 January 2014

Downloaded by [University of Toledo], [K. A. Shamaileh] at 09:18 24 January 2014

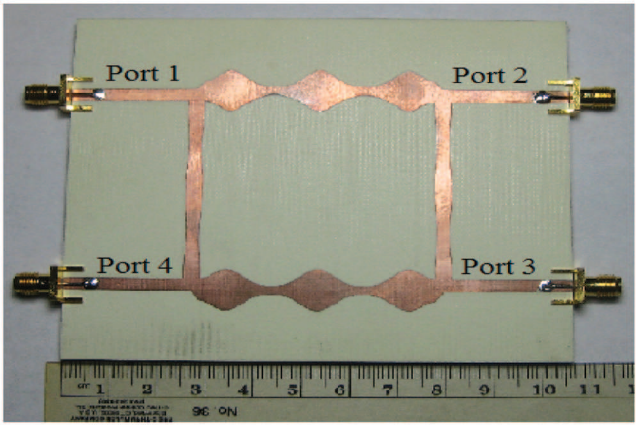

Figure 4. Photograph of fabricated dual-band 3-dB 90° BLC.

Figure 4 shows a photograph of the fabricated dual-band coupler, while Figure 5 shows the full-wave simulation results. As can be seen from Figure 5(a), simulation results indicate that the input port matching parameter (S_{11}) is below −20 and −18 dB at 0.83 and 2.4 GHz, respectively, and the obtained experimental results using an Agilent E5071B vector network analyzer (VNA) are in good agreement with the resulting simulations.

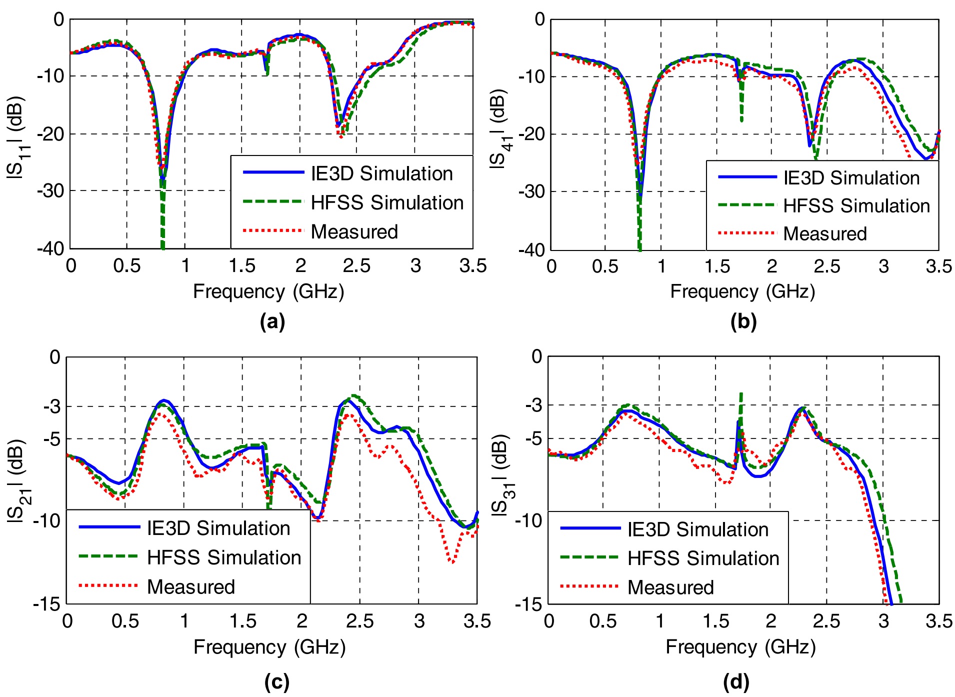

Figure 5. Simulation and measurement results for dual-band 3-dB 90° BLC: (a) input port matching parameter (S_{11}) (b) isolation parameter (S_{41}), (c) transmission parameter (S_{21}), and (d) transmission parameter (S_{31}).

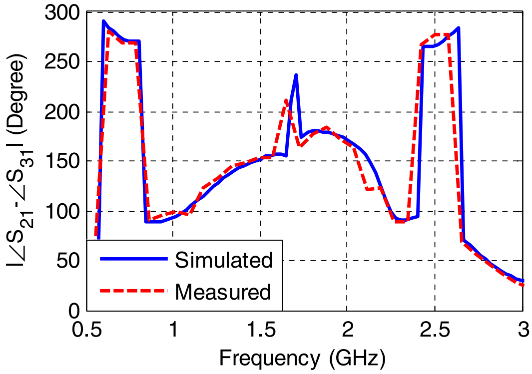

Figure 6. Simulated and measured phase difference between S_{21} and S_{31}.

Moreover, the isolation parameter S_{41} is below −20 dB at the design frequencies, as shown in Figure 5(b). The simulated transmission parameter S_{21}, shown in Figure 5(c), is equal to −2.9 and −2.7 dB at the first and second bands, respectively, which are very close to the theoretical value of −3 dB, whereas the results obtained from measurement are around −3.4 dB. Furthermore, Figure 5(d) shows the simulated transmission parameter S_{31}, which equals −3.4 dB at 0.9 and 2.4 GHz. Those values are also close to −3 dB, whereas the measured results are −3.5 dB in proximity to the two design frequencies. It is worth pointing out here that the slight discrepancies between the simulated and measured results are thought to be due to connector losses as well as measurement errors.

Figure 6 shows the magnitude of the measured phase difference between the transmission parameters, S_{21} and S_{31}. As expected, a phase difference of $90 \pm 5°$ can be clearly discerned at the two design frequencies, 0.9 and 2.4 GHz.

Figure 7 illustrates the simulated current distributions at an arbitrarily selected in-band frequency of 0.86 GHz and out-of-band frequency of 1.5 GHz. It can be seen that at the in-band frequency (Figure 7(a)), there are weak current distributions at port 4, which confirms the proper operation of the proposed coupler as the isolation port possesses

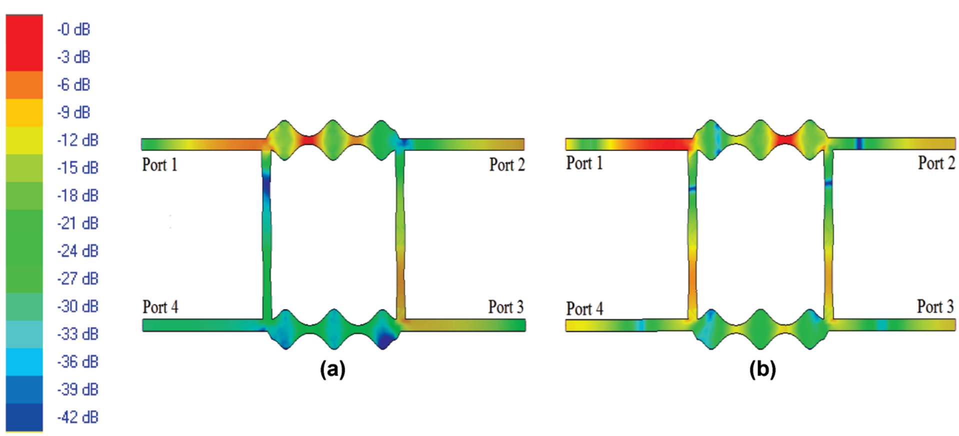

Figure 7. Current distribution of dual-band 3-dB 90° BLC: (a) in-band frequency (0.86 GHz) and (b) out-of-band frequency (1.5 GHz).

Downloaded by [University of Toledo], [K. A. Shamaileh] at 09:18 24 January 2014

high impedance at such a frequency. On the contrary, relatively higher electric currents are concentrated along the isolation port at the out-of-band frequency (Figure 7(b)).

3.2. *Triple-Band 3-dB BLC*

After the successful implementation of the dual-band NTL BLC, a triple-band coupler was implemented in a similar fashion to prove the validity, repeatability, and robustness of the underlying design procedure. The proposed triple-band NTL BLC is designed to operate at three concurrent frequencies, specifically, 0.9, 2.4, and 5.4 GHz. Such bands find many applications in modern wireless communications, such as GSM, WLAN, WiFi, and WiMAX technologies. Considering the same previously mentioned substrate, two NTLs—$Z_1(z)$ and $Z_2(z)$ with widths 1 mm $< W_1(z) <$ 5.5 mm and 1 mm $< W_2(z) <$ 10 mm, respectively—are designed with lengths d_1 and d_2 of 25.18 and 49.27 mm, respectively, which equals $\lambda/8$ and $\lambda/4$ at the lowest design frequency (i.e., 0.9 GHz), whereas the characteristic impedances Z_{o1}, Z_{o2}, and Z_o are chosen to be 50, 35, and 50 Ω, respectively. Similar to the dual-band design, K_1, K_2, and N are set to 50, 50, and 10, respectively. The error value from the optimization process was 0.026. Table 2 shows the obtained Fourier series coefficients for $Z_1(z)$ and $Z_2(z)$.

Figure 8 shows a photograph of the implemented triple-band BLC, whereas Figure 9 represents the simulated and measured response of the corresponding S-parameters. As can be seen from Figures 9(a) and 9(b), the simulated input matching and isolation parameters are both below −20 dB at the design frequencies, and the measured results are in very good agreement with the simulated ones. Moreover, the simulated transmission parameters (S_{21} and S_{31}) are in the ranges of −2.5 to −3.5 dB, −2.5 to −3.6 dB, and −3.4 to −4 dB at 0.86, 2.44, and 5.48 GHz, respectively. Furthermore, measured results in the ranges of −3.1 to −3.6 dB, −3.4 to −4.5 dB, and −4.3 to −4.6 dB were obtained at the first, second, and third bands, respectively. The slight frequency shifts, as well as

Table 2
Fourier coefficients for variable impedance profiles in triple-band BLC design

Fourier coefficients for $Z_1(z)$					
C_0	C_1	C_2	C_3	C_4	C_5
0.1782	0.1954	0.2223	−0.2163	−0.0881	−0.0589
C_6	C_7	C_8	C_9	C_{10}	
−0.0540	−0.0487	−0.0450	−0.0432	−0.0418	
Fourier coefficients for $Z_2(z)$					
C_0	C_1	C_2	C_3	C_4	C_5
0.1680	0.1112	0.3284	−0.0909	0.2555	−0.2732
C_6	C_7	C_8	C_9	C_{10}	
−0.1565	−0.0920	−0.0933	−0.0783	−0.0790	

Downloaded by [University of Toledo], [K. A. Shamaileh] at 09:18 24 January 2014

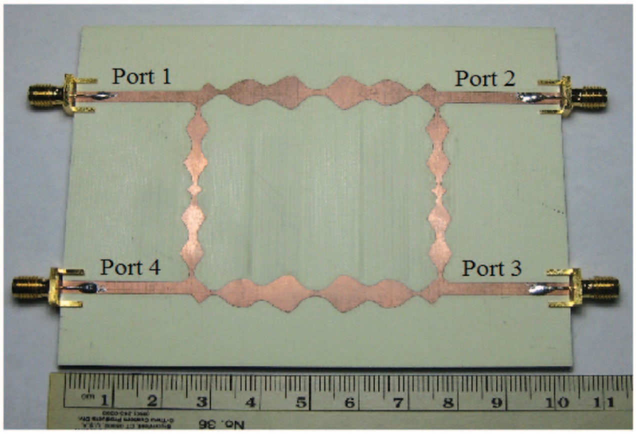

Figure 8. Photograph of fabricated triple-band 3-dB 90° BLC.

the increased losses, are thought to be due to the resulting optimization error, different types of losses, and measurement errors.

Figure 10 illustrates the simulated and measured phase difference between the two output ports. It can be clearly seen that a phase shift of 90 ± 7° occurs around the design frequencies (i.e., 0.9, 2.4, and 5.4 GHz).

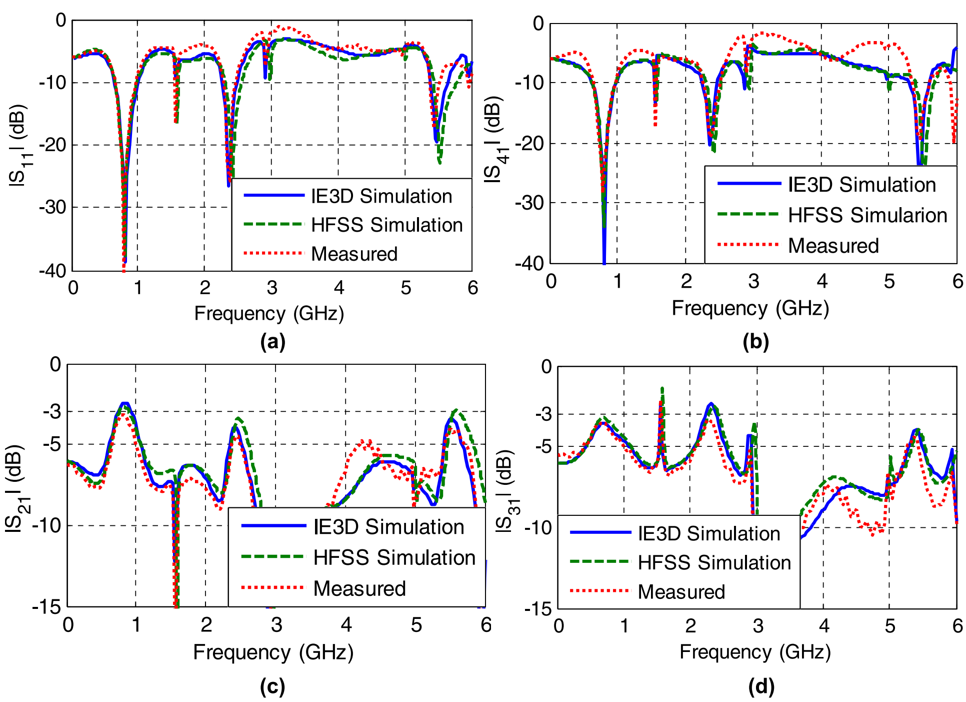

Figure 9. Simulation and measured results for triple-band 3-dB 90° BLC: (a) input port matching parameter (S_{11}), (b) isolation parameter (S_{41}), (c) transmission parameter (S_{21}), and (d) transmission parameter (S_{31}).

Downloaded by [University of Toledo], [K. A. Shamaileh] at 09:18 24 January 2014

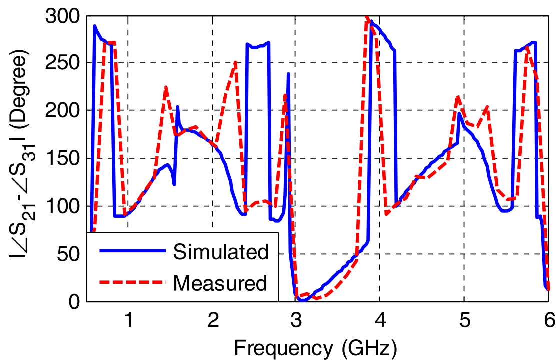

Figure 10. Simulated and measured phase difference between S_{21} and S_{31}.

4. Conclusions

In this article, a new approach for the design of multi-band BLCs is investigated to overcome realization difficulties that are often encountered with conventional BLCs. Based on the NTL theory, an efficient technique for the design of multi-frequency 3-dB BLCs is proposed. Each uniform transmission line in the conventional BLC is replaced with a single NTL exhibiting a Fourier-based profile. Even- and odd-mode analysis and an optimization-driven process are carried out to achieve the desired response at the design frequencies. To justify the design principle, dual- and triple-band BLCs suitable for various modern wireless applications were designed, fabricated, and measured. The agreement between both simulated and measured results proves the design methodology.

Funding

This work has been supported by the National Science Foundation through an Engineering Design and Innovation grant (no. 1000744).

References

Ansys, Inc. 2011. *ANSYS high frequency structure simulator (HFSS)*. Canonsburg, PA.

Cheng, K.-K., & F.-L. Wong. 2004. A novel approach to the design and implementation of dual-band compact planar 90° branch-line coupler. *IEEE Trans. Microw. Theory Tech.* 52:2458–2463.

Cheng, K.-K., & S. Yeung. 2012. A novel dual-band 3-dB branch-line coupler design with controllable bandwidths. *Trans. Microw. Theory Tech.* 60:3055–3061.

Chin, K.-S., K.-M. Lin, Y.-H. Wei, T.-H. Tseng, & Y.-J. Yang. 2010. Dual-band branch-line and rat-race couplers with stepped-impedance-stub lines. *IEEE Trans. Microw. Theory Tech.* 58:1213–1221.

Jung, S.-C., R. Negra, & F. Ghannouchi. 2009. A miniaturized double-stage 3dB broadband branch-line hybrid coupler using distributed capacitors. *Proceedings of Asia Pacific Microwave Conference (APMC)*, Singapore, 7–10 December, 1323–1326.

Khalaj-Amirhosseini, M. 2006. Wideband or multiband impedance matching using microstrip non-uniform transmission lines. *Prog. Electromagn. Res.* 66:15–25.

Khalaj-Amirhosseini, M. 2008. Non-uniform transmission lines as compact uniform transmission lines. *Prog. Electromagn. Res. C* 4:205–211.

Lee, H., & S. Nam. 2007. Triband branch line coupler using double-Lorentz transmission lines. *Microw. Opt. Technol. Lett.* 50:1174–1177.

Downloaded by [University of Toledo], [K. A. Shamaileh] at 09:18 24 January 2014

Li, Y. 1993. *Centering, trust region, reflective techniques for nonlinear minimization subject to bounds*. Technical Report 93-1385, Cornell University, NY.

Lin, F., Q.-X. Chu, & Z. Lin. 2010. A novel tri-band branch-line coupler with three controllable operating frequencies. *IEEE Microw. Wirel. Compon. Lett.* 20:666–668.

Liou, C.-Y., M.-S. Wu, J.-C. Yeh, Y.-Z. Chueh, & S.-G. Mao. 2009. A novel triple-band microstrip branch-line coupler with arbitrary operating frequencies. *IEEE Microw. Wirel. Compon. Lett.* 19:683–685.

Mentor Graphics PCB Design Software. 2006. *IE3D: Method of moment (MoM) based full-wave electromagnetics simulator, v. 14.2*. Wilsonville, OR.

Park, M.-J. 2009. Dual-band, unequal length branch-line coupler with center-tapped stubs. *IEEE Microw. Wireless Compon. Lett.* 19:617–619.

Piazzon, L., P. Saad, P. Colantonio, F. Giannini, K. Andersson, & C. Fager. 2012. Branch-line coupler design operating in four arbitrary frequencies. *IEEE Microw. Wirel. Compon. Lett.* 22:67–69.

Pozar, D. 2005. *Microwave engineering*, 3rd ed., chaps. 4 & 7. New York: Wiley.

Rawat, K., M. Rawat, M.-S. Hashmi, & F.-M. Ghannouchi. 2013. Dual-band branch-line hybrid with distinct power division ratio over the two bands. *Int. J. RF Microw. Comp. Aid. Eng.* 23:90–98.

Sinchangreed, V., M. Uthansakul, & P. Uthansakul. 2011. Design of tri-band quadrature hybrid coupler for WiMAX applications. *Proceedings of International Symposium on Intelligent Signal Processing and Communication Systems (lSPACS)*, Chiang Mai, Thailand, 7–9 December, 1–4.

Tanigawa, S., K. Hayashi, T. Fujii, T. Kawai, & I. Ohta. 2007. Tri-band/broadband matching techniques for 3-dB branch-line couplers. *Proceedings of 37th European Microwave Conference*, Munich, Germany, 9–12 October, 560–563.

Yeung, L. 2011. A compact dual-band 90° coupler with coupled-line sections. *IEEE Trans. Microw. Theory Tech.* 59:2227–2232.

Downloaded by [University of Toledo], [K. A. Shamaileh] at 09:18 24 January 2014